



# Sulfur speciation monitored *in situ* with solid state gold amalgam voltammetric microelectrodes: polysulfides as a special case in sediments, microbial mats and hydrothermal vent waters†‡

George W. Luther, III,\*<sup>a</sup> Brian T. Glazer,<sup>a</sup> Laura Hohmann,<sup>a</sup> Jeannette I. Popp,<sup>a</sup> Martial Taillefert,<sup>a</sup> Timothy F. Rozan,<sup>a</sup> Paul J. Brendel,<sup>c</sup> Stephen M. Theberge<sup>a§</sup> and Donald B. Nuzzio<sup>d</sup>

<sup>a</sup>College of Marine Studies, University of Delaware, Lewes, DE 19958, USA.

E-mail: [luther@udel.edu](mailto:luther@udel.edu)

<sup>b</sup>School of Earth & Atmospheric Sciences, Georgia Institute of Technology, 221 Bobby Dodd Way, Atlanta, GA 30332-0340, USA

<sup>c</sup>Ward Melville High School, 380 Old Town Road, East Setauket, NY 11733, USA

<sup>d</sup>Analytical Instrument Systems, Inc., 1059C Old York Road, Ringoes, NJ 08851, USA

Received 8th August 2000, Accepted 24th October 2000

First published as an Advance Article on the web 6th December 2000

Sulfur speciation was determined in real time in salt marsh microbial mats, subtidal sediments and hydrothermal vent diffuse flow waters using solid state gold-amalgam voltammetric microelectrodes. Chemical species were measured *in situ* without any sample manipulation or processing. The partially oxidized sulfur species detected were polysulfides, thiosulfate, elemental sulfur and tetrathionate. Fe(III) oxidation of hydrogen sulfide does not occur within the mats where microbially mediated processes are responsible for oxidation of H<sub>2</sub>S. In sediments and diffuse flow vent waters, Fe(III) phases are the direct oxidant of H<sub>2</sub>S. Sulfur speciation determined in this work is due to *in situ* biogeochemical processes and is not due to artefacts of sample manipulation. The voltammetric data show that polysulfides are the first detectable intermediate during sulfide oxidation which is consistent with previous laboratory studies.

## Introduction

*In situ* measurements are necessary to understand dynamic environments where speciation can change in seconds as a result of chemical, biological and physical processes. A wide range of natural environments produce hydrogen sulfide that can then be oxidized back to sulfate by oxygen, iron(III) and manganese(III,IV) compounds.<sup>1–5</sup> The oxidation may be abiotic or bacterially mediated and occur at reasonable rates (minutes to hours).<sup>1–5</sup> The oxidation of sulfide frequently leads to intermediate oxidation state compounds, such as elemental sulfur, polysulfides and thiosulfate<sup>4,5</sup> which may be used by bacteria<sup>6</sup> or may react with metals<sup>7</sup> and organic compounds.<sup>8,9</sup> Using the mercury electrode and/or the gold amalgam microelectrode it is possible to measure a variety of soluble sulfur compounds and ions including hydrogen sulfide, polysulfides, thiosulfate, aqueous iron monosulfide, elemental sulfur, tetrathionate and organic thiols.<sup>10–16</sup>

Polysulfides are key intermediates in the oxidation of H<sub>2</sub>S but could not be easily measured or even identified *in situ* until recently.<sup>16</sup> Previous studies have used a dropping Hg electrode to measure polysulfides discreetly.<sup>10,17</sup> In addition, most previous measurements of sulfur species were determined after sample manipulation. Sample manipulation includes: (i) taking a water sample in Niskin or Go-Flo bottles and measuring the speciation back in the lab (either at home or onboard ship); and (ii) taking sediment cores which are then cut into sections (typically >3 mm), centrifuged for removal,

filtration and measurement of the porewater. Sample processing can mix oxidized sediments/waters and reduced sediments/waters which can react to create sulfur species of intermediate oxidation state. Although the measurements are performed well, the sample processing causes artefacts which can complicate the interpretation of what biogeochemical processes occur in the field. Thus, the exact determination of polysulfides, which appear to be the first formed or detected intermediates in sulfide oxidation,<sup>4,5</sup> has been hampered.

In this work, we describe the electrode reactions and quantify the presence and/or absence of these species over space and time in microbial mats, sediments and hydrothermal vent fields using a solid state gold amalgam voltammetric microelectrode.<sup>18</sup> The electrodes have (sub)millimetre vertical resolution in mats and sediments. The initial survey work that is presented here will show *in situ* sulfur speciation measurements where: (1) the electrodes and a portable analyzer have been brought into the field for analysis of salt marsh microbial mats; (2) subtidal sediment cores have been collected and returned to the laboratory for electrode insertion; and (3) waters at 2500 m depth have been analyzed with a submersible *in situ* analyzer from a deep sea submarine (DSV *Alvin*). Artefacts caused by sample processing are minimized and a correct assessment of the sulfur speciation including the presence of polysulfides can be made.

## Experimental

A standard three electrode cell was used in all experiments. The working electrode was a gold amalgam (Au/Hg) electrode of 100 μm diameter. The electrode was made in glass or commercially available PEEK<sup>®</sup> (polyethyl ether ketone) tubing depending on the application as per Luther *et al.*<sup>19</sup> Glass was used for the bacterial mat and sediment analyses

†Presented at the Whistler 2000 Speciation Symposium, Whistler Resort, BC, Canada, June 25–July 1, 2000.

‡Electronic Supplementary Information available. See <http://www.rsc.org/suppdata/em/b0/b006499h/>

§Present address: Dept. of Chemistry, Merrimack College, 315 Turnpike Street, N. Andover, MA 01845, USA.

because 5 mm glass could be extruded to about 0.2–0.3 mm for ease of insertion into the environmental sample.

Microbial mats from Great Marsh, Delaware, during July 6, 2000, were analyzed *in situ* with a gold amalgam (Au/Hg) microelectrode which was inserted into the mat with a manually controlled three-axis Narshige micromanipulator. The counter (Pt) and reference (Ag/AgCl in saturated KCl) electrodes were placed in water overlying the mat so they did not enter the sediment or sulfide zone. A battery operated DLK 100A from Analytical Instrument Systems, Inc. was used for all electrochemical analyses. The overlying water had a salinity of 32 at 29.6 °C and a pH of 8.29 so that O<sub>2</sub> saturation is 198.9 μmol dm<sup>-3</sup>. There was no cloud cover during the experiment, which occurred between 1200 and 1400 h.

For subtidal sediment analyses, cores were obtained at an ambient temperature (15–20 °C), returned to the laboratory and placed in a water bath/incubator for insertion of the gold amalgam (Au/Hg) microelectrode. The reference electrode was a standard Ag/AgCl as above and the counter-electrode was Pt wire. The area chosen for study was northwest Rehoboth Bay of southern Delaware.

For hydrothermal vent research at 9° N East Pacific Rise during May 1999, a Delrin tube was made to hold up to four PEEK<sup>®</sup> electrodes and two glass electrodes with a thermocouple and Teflon tubing to suck water into syringes using the SIPPER sampler.<sup>20</sup> The lower end of this tube had set screws to hold the working electrodes stationary in the tube. The working electrodes were recessed at the lower end of the wand to protect the tips of the electrodes from losing the Hg film. The lower end also had feet to allow water flow across the electrode surface. The top end of the tube was mated *via* four stainless steel nuts and bolts to a large diameter tube. Inserted between these lower and upper Delrin tubes was a steel handle for DSV *Alvin's* arm to pick up the entire wand assembly for deployment of the electrodes. We refer to this as a sensor package for simplicity. The reference electrode was Ag/AgCl and the counter-electrode was Pt wire, both of which were mounted on the basket of DSV *Alvin* so that they would not enter sulfidic waters. For hydrothermal vent work, the Ag/AgCl reference was silver wire which was oxidized in seawater at +9 V for 10 s to form a AgCl coating; the electrode was used as a solid state electrode in the seawater medium ( $I=0.7$ ) so that no pressure effects on filling solutions would hinder electrode performance. Comparison of peak potentials for the analytes measured *in situ* and onboard ship were the same and were similar to those for a saturated calomel electrode (SCE). The sensor package was held over areas at the base of vent chimneys where the vent tubeworm, *Riftia pachyptila*, inhabits. These areas are termed diffuse flow because water temperatures are less than 25 °C and do not emanate from the vent orifice. A submersible electrochemical analyzer from Analytical Instrument Systems, Inc. was used for data collection.

Electrochemically conditioning the electrode between scans removes any chemical species from the electrode surface restoring it for use for the next measurement. To remove any previously deposited Fe and Mn; the working electrode was conditioned at a potential of -0.1 V for 10 s.<sup>18</sup> The voltage range scanned was from -0.1 V to -2.0 V for linear sweep voltammetry (LSV) and for cyclic voltammetry (CV). In LSV or CV, the scan rate was either 200, 500 or 1000 mV s<sup>-1</sup>. In square wave voltammetry (SWV), the following set of parameters was used: pulse height, 24 mV; step increment, 1 mV; frequency, 100 Hz; scan rate, 200 mV s<sup>-1</sup>. LSV and CV were used primarily to measure O<sub>2</sub> and sulfur species. SWV was employed for analysis of the metal redox species.

Standard calibration curves were produced in seawater over the temperature range of the samples for all sulfur species and the electrodes calibrated as per Brendel and Luther.<sup>18</sup> Pure Na<sub>2</sub>S<sub>4</sub> was prepared by premixing and heating elemental sulfur and anhydrous sodium sulfide in sealed and evacuated glass

tubes.<sup>7</sup> The purity of the product was confirmed by differential scanning calorimetry (DSC) analysis and the products are typically >99% pure. Individual standard solutions of sulfide and thiosulfate were made using ACS reagent grade Na<sub>2</sub>S·9H<sub>2</sub>O (Aldrich) and Na<sub>2</sub>S<sub>2</sub>O<sub>3</sub>·5H<sub>2</sub>O (Fisher). Solutions of S<sup>0</sup> were prepared by dissolving 99.998% pure elemental sulfur (Aldrich) in HPLC grade methanol. S<sup>0</sup> standards were then diluted to 0.001% v/v CH<sub>3</sub>OH·H<sub>2</sub>O to minimize any potential organic fouling of the Hg electrode. All laboratory prepared solutions were made with Milli-Q water that had been purged with N<sub>2</sub> for 1 h. The N<sub>2</sub> was first passed through a pyrocatechol trap, which lowers O<sub>2</sub> concentrations <0.2 μmol dm<sup>-3</sup>.

## Results and discussion

### Sulfur species

Table 1 shows many of the redox compounds and ions including some of the sulfur species that can be measured with a Au/Hg electrode. Sulfide oxidation results in formation of polysulfides, elemental sulfur, thiosulfate, sulfite and polythionates (*e.g.*, tetrathionate) in lab studies<sup>1–5</sup> but the possible existence of these sulfur intermediates has only been confirmed in a few field studies.<sup>10,11,13–16</sup> Sulfite can be measured<sup>10</sup> at pH values <6, which are not common in microbial mats and sediments where the pH is >7. All sulfur species give one peak except for polysulfides. At slow scan speeds, H<sub>2</sub>S, S<sub>8</sub> and polysulfides (S<sub>x</sub><sup>2-</sup>) overlap to give one peak at about -0.60 V and the sum of all their contributions is termed S<sub>red</sub>.<sup>10,13–17</sup> However, S<sub>x</sub><sup>2-</sup> are unique because they exist in two oxidation states and it is possible to discriminate each oxidation state with fast potential scans.<sup>16</sup> At positive potentials, S<sub>x</sub><sup>2-</sup> react to form a HgS<sub>x</sub> species at the Au/Hg electrode, which is an electrochemical oxidation of the Hg. On scanning negatively, HgS<sub>x</sub> is reduced to Hg and S<sub>x</sub><sup>2-</sup> at a more positive potential that overlaps with H<sub>2</sub>S and S<sub>8</sub>, then the (x-1)S<sup>0</sup> atoms are reduced to sulfide at a more negative potential. Because the reduction of S<sup>0</sup> atoms in S<sub>x</sub><sup>2-</sup> is an irreversible process, increasing the scan rate shifts that peak to more negative potentials and permits separation of the HgS<sub>x</sub> reduction from the S<sub>8</sub> reduction [Fig. 1; Table 1, eqns. (4a)–(4c)].<sup>16,21</sup> The peaks can be fully resolved at scan rates of 1000 mV s<sup>-1</sup>. On the positive scan in the polysulfide CV, all the S<sup>0</sup> that was reduced to sulfide and the S<sup>2-</sup> in the polysulfide react to reform a HgS film (termed S<sub>AVS</sub>). Lastly, an irreversible peak for the reduction of Fe<sup>2+</sup> in soluble FeS, FeS<sub>aq</sub>, can be observed at -1.10 V.<sup>12</sup>

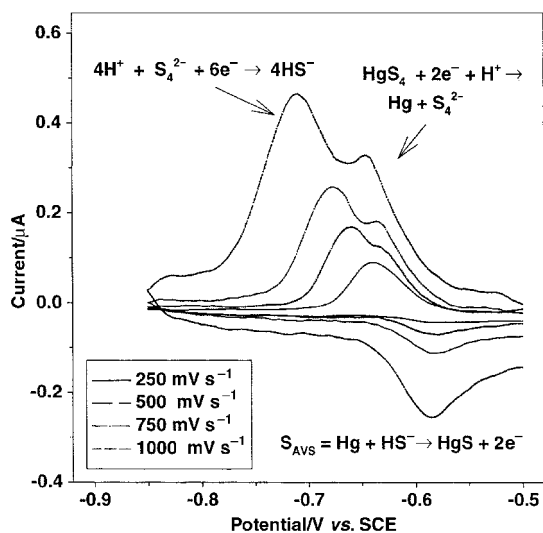
### *In situ* mat work

Fig. 2 shows representative voltammograms taken from a microbial mat in Great Marsh Delaware. Scan A clearly shows the existence of only oxygen above the mat (4 mm) whereas scan B shows a significant signal due to H<sub>2</sub>O<sub>2</sub> at 0–2 mm above the mat. The H<sub>2</sub>O<sub>2</sub> signal is normally equal to the O<sub>2</sub> signal because, at the Hg electrode, O<sub>2</sub> reduces to H<sub>2</sub>O<sub>2</sub> [Table 1, eqns. (1a)–(1b)] which in turn reduces to H<sub>2</sub>O. Peroxide has been shown to exist in significant quantities in biofilms.<sup>22</sup> Scan C shows two peaks: one for thiosulfate, S<sub>2</sub>O<sub>3</sub><sup>2-</sup> ( $E_{1/2} = -0.15$  V), and S<sub>red</sub> ( $E_{1/2} = -0.60$  V) at 2 mm below the mat surface. Fast scans of 1000 mV s<sup>-1</sup> only show one peak indicating that polysulfides are not present as part of S<sub>red</sub>. Thus, S<sub>red</sub> in this case is composed of soluble S<sub>8</sub> because this upper part of the mat is more oxidized due to the oxygen gradient. Deeper into the mat (5 mm), scan D, shows a clear double peak at  $E_{1/2} = -0.58$  V and -0.68 V indicative of polysulfide formation. The more positive signal is due to S<sup>2-</sup> sulfur from H<sub>2</sub>S and S<sub>x</sub><sup>2-</sup> and the more negative signal is due to S<sup>0</sup> sulfur from S<sub>x</sub><sup>2-</sup>. Polysulfides persist in the bottom portion

**Table 1** Relevant sulfur and iron species electrode reactions at the Au/Hg electrode vs. the SCE at 25 °C <sup>a</sup>

		$E_p/V$	MDL/ $\mu\text{mol dm}^{-3}$
(1a)	$\text{O}_2 + 2\text{H}^+ + 2\text{e}^- \rightarrow \text{H}_2\text{O}_2$	-0.30	5
(1b)	$\text{H}_2\text{O}_2 + 2\text{H}^+ + 2\text{e}^- \rightarrow \text{H}_2\text{O}$	-1.3	5
(2a)	$\text{HS}^- + \text{Hg} \rightarrow \text{HgS} + \text{H}^+ + 2\text{e}^-$	Adsorption onto Hg < -0.60	
(2b)	$\text{HgS} + \text{H}^+ + 2\text{e}^- \leftrightarrow \text{HS}^- + \text{Hg}$	~ -0.60	<0.2
(3a)	$\text{S}^0 + \text{Hg} \rightarrow \text{HgS}$	Adsorption onto Hg < -0.60	
(3b)	$\text{HgS} + \text{H}^+ + 2\text{e}^- \leftrightarrow \text{HS}^- + \text{Hg}$	~ -0.60	<0.2
(4a)	$\text{Hg} + \text{S}_x^{2-} \rightarrow \text{HgS}_x + 2\text{e}^-$	Adsorption onto Hg < -0.60	
(4b)	$\text{HgS}_x + 2\text{e}^- \leftrightarrow \text{Hg} + \text{S}_x^{2-}$	~ -0.60	<0.2
(4c)	$\text{S}_x^{2-} + x\text{H}^+ + (2x-2)\text{e}^- \rightarrow x\text{HS}^-$	~ -0.60	<0.2
(5)	$2\text{RSH} \leftrightarrow \text{Hg}(\text{SR})_2 + 2\text{H}^+ + 2\text{e}^-$	Typically more positive than $\text{H}_2\text{S}/\text{HS}^-$	
(6)	$2\text{S}_2\text{O}_3^{2-} + \text{Hg} \leftrightarrow \text{Hg}(\text{S}_2\text{O}_3)_2^{2-} + 2\text{e}^-$	-0.15	16
(7)	$\text{S}_4\text{O}_6^{2-} + 2\text{e}^- \rightarrow 2\text{S}_2\text{O}_3^{2-}$	-0.45	15
(8)	$\text{FeS} + 2\text{e}^- + \text{H}^+ \rightarrow \text{Fe}(\text{Hg}) + \text{HS}^-$	-1.1	Molecular species
(9)	$\text{Fe}^{2+} + \text{Hg} + 2\text{e}^- \leftrightarrow \text{Fe}(\text{Hg})$	-1.43	15
(10)	$\text{Fe}^{3+} + \text{e}^- \leftrightarrow \text{Fe}^{2+}$	-0.2 to -0.9 V	Molecular species

<sup>a</sup>Potentials versus the Ag/AgCl are 44 mV more positive. All data were obtained with a 100  $\mu\text{m}$  diameter electrode ( $A = 7.85 \times 10^{-3} \text{ mm}^2$ ).  $\text{O}_2$  data were collected by LSV at  $200 \text{ mV s}^{-1}$ ; all others were collected by SWV at  $200 \text{ mV s}^{-1}$ . Potentials can vary with scan rate and concentration; e.g., on increasing concentration, the sulfide signal becomes more negative.<sup>7,16</sup> When applying potential from a positive to negative scan direction, sulfide and  $\text{S}^0$  react in a two step process (1, adsorption onto the Hg surface; 2, reduction of the HgS film) and polysulfides react in a three step process (1, adsorption onto the Hg surface; 2, reduction of the  $\text{HgS}_x$  film; 3, reduction of the  $\text{S}^0$  in the polysulfide). Increasing the scan rate separates electrode reactions (4b) and (4c) into two peaks because eqn. (4c) is an irreversible process (increasing scan rate shifts this signal<sup>21</sup>). MDL = minimum detection limit.



**Fig. 1** Separation of the tetrasulfide signal into  $\text{S}^0$  and  $\text{S}^{2-}$  signals as scan rate is increased. At the  $1000 \text{ mV s}^{-1}$  scan rate, two signals are readily observable with a ratio of 3 : 1 for  $\text{S}^0$  to  $\text{S}^{2-}$  with an increase in signal intensity as expected. These data were obtained with a hanging Hg drop electrode.

of the mat where purple sulfur bacteria exist. As the bottom of the mat is penetrated and the sediment is reached, only one peak at  $E_{1/2} = -0.58 \text{ V}$  is observed in scan E (1.5 mm below the mat/sediment interface), which indicates only  $\text{H}_2\text{S}/\text{HS}^-$  is present. Traces of  $\text{FeS}_{\text{aq}}$  are noted in scan E and other scans

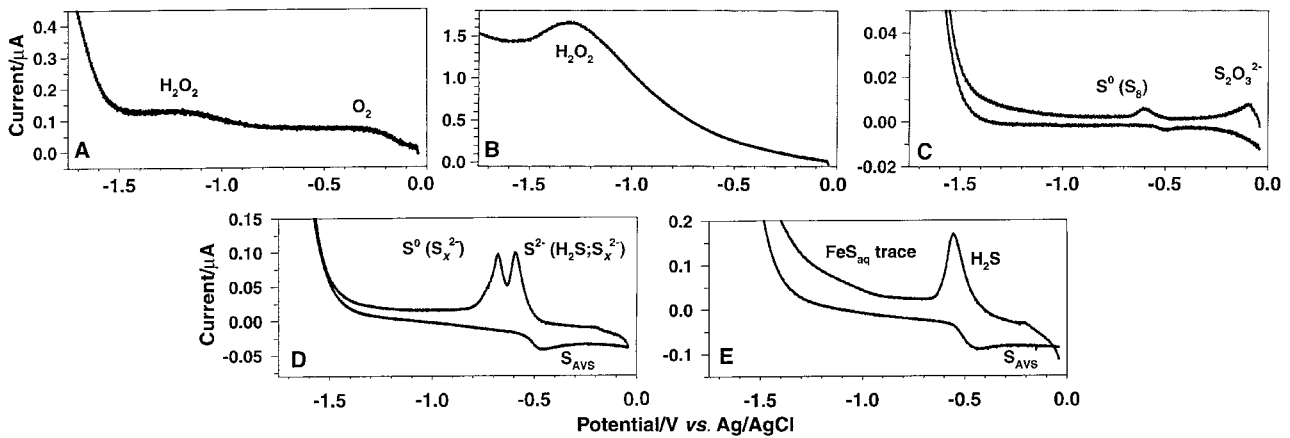
deeper into the sediment (data not shown). In none of these scans is there evidence for dissolved Fe and Mn in the mat.

Fig. 3 shows a profile of oxygen and sulfur species into the mat which is about 7 mm thick. The  $\text{O}_2$  profile is typical for microbial mats.<sup>23-26</sup>  $\text{O}_2$  in the water column reaches a maximum above the mat/water interface as in previous studies. During the day,  $\text{O}_2$  increases due to oxygenic photosynthesis and creates the levels of (super)saturation (~200%) shown in Fig. 3. These levels drive the much larger  $\text{O}_2$  fluxes from the surface of the mat into the water column, thus forming a maximum at or slightly above the mat/water interface. However, as the mat/water interface was reached,  $\text{H}_2\text{O}_2$  an intermediate in  $\text{O}_2$  formation via water splitting was observed. Previous microelectrode studies using membrane electrodes rather than solid state electrodes could not determine if  $\text{H}_2\text{O}_2$  was present, but solid state microelectrodes used in biofilm work<sup>22</sup> have shown the presence of peroxide.

These data clearly show that there is a redox transition between the overlying water, the mat and the sediment as expected. The transition from reduced sulfide below the mat to partially oxidized sulfur species ( $\text{S}_x^{2-}$ ) in the center of the mat to more oxidized sulfur species towards the top of the mat can be explained by the biology and chemistry of the mat. Table 2 shows a schematic representation of the chemistry of a microbial mat. Visual inspection indicated that green algae/cyanobacteria (6 mm thick), which produce  $\text{O}_2$  and organic matter during photosynthesis, inhabited the top of the mat (7 mm total thickness). Underneath the algae were purple sulfur bacteria (PSB; 1 mm thick) which use  $\text{H}_2\text{S}$  to produce  $\text{S}_8$  ( $\text{S}^0$ ) and organic matter. The organic matter from the cyanobacteria and purple sulfur bacteria is the fuel for dissimilatory sulfate reducing bacteria which lie in the

**Table 2** Redox reactions that form chemical gradients within the microbial mat environment

Process	Reaction	Pathway
Oxygenic photosynthesis	$\text{CO}_2 + \text{H}_2\text{O} \rightarrow \text{CH}_2\text{O} + \text{O}_2$	Algae/cyanobacteria
Anoxygenic photosynthesis	$\text{CO}_2 + 2\text{H}_2\text{S} \rightarrow \text{CH}_2\text{O} + \text{H}_2\text{O} + 2\text{S}^0$	Purple sulfur bacteria
Sulfate reduction	$2(\text{CH}_2\text{O}) + \text{SO}_4^{2-} \rightarrow 2\text{HCO}_3^- + \text{H}_2\text{S}$	Sulfate reducing bacteria
Fe chemistry	$2\text{Fe}^{3+} + \text{H}_2\text{S} \rightarrow 2\text{Fe}^{2+} + 2\text{H}^+ + \text{S}^0 (\text{S}_x^{2-})$ $\text{Fe}^{2+} + \text{H}_2\text{S} \rightarrow \text{FeS} + 2\text{H}^+$ $\text{Fe}^{2+} + \text{S}_x^{2-} \rightarrow \text{FeS} + (x-1)\text{S}_8$ $\text{FeS} + \text{H}_2\text{S} \rightarrow \text{FeS}_2 + \text{H}_2$	Chemical reaction
Sulfur oxidation	$2\text{H}_2\text{S} + \mu\text{O}_2 + \text{Fe}^{2+} \rightarrow$ $\text{H}_2\text{S} + \text{Fe}^{3+} \rightarrow$	Chemical reaction and/or sulfur oxidizing bacteria
	$\text{S}_2\text{O}_3^{2-}; \text{S}_8; \text{S}_x^{2-}; \text{SO}_3^{2-}; \text{SO}_4^{2-}; \text{S}_4\text{O}_6^{2-}$	



**Fig. 2** Representative LSV and CV scans showing sulfur speciation from a salt marsh microbial mat. A, LSV of  $500 \text{ mV s}^{-1}$  scan rate showing  $\text{O}_2$  in overlying water; B, LSV of  $500 \text{ mV s}^{-1}$  scan rate showing  $\text{H}_2\text{O}_2$  at the mat/water interface; C, CV of  $1000 \text{ mV s}^{-1}$  scan rate showing  $\text{S}_8$  and  $\text{S}_2\text{O}_3^{2-}$  as the electrode penetrates through the green algae section; D, CV of  $1000 \text{ mV s}^{-1}$  scan rate showing  $\text{S}_x^{2-}$  signals from  $\text{S}^0$  and  $\text{S}^{2-}$ ; E, CV of  $1000 \text{ mV s}^{-1}$  scan rate showing only  $\text{H}_2\text{S}$  and a trace of  $\text{FeS}_{\text{aq}}$  as the electrode penetrates the sediment.

sediments underneath the PSB. Although the sediments contain significant quantities of solid phase  $\text{Fe(II,III)}$  which react with sulfide to form  $\text{FeS}$  and  $\text{FeS}_2$ , we did not observe a significant signal for  $\text{FeS}_{\text{aq}}$  in this mat.  $\text{FeS}_{\text{aq}}$  is found readily in the black colored sediments.

The mat surface produces oxidants,  $\text{O}_2$  and  $\text{H}_2\text{O}_2$ , which are able to oxidize sulfur compounds whereas the PSB mediate sulfide oxidation directly. The formation of  $\text{S}_8$  and  $\text{S}_2\text{O}_3^{2-}$  at the upper portions of the mat is consistent with the stronger oxidizing characteristics of that section of the mat where oxygenic photosynthesis occurs. Polysulfides form in the

interior of the mat and their formation likely occurs from the reaction of  $\text{HS}^-$  with  $\text{S}_8$  that PSB produce during anoxygenic organic matter production. The formation of these partially oxidized sulfur species is the result of the oxidation of  $\text{H}_2\text{S}/\text{HS}^-$  which diffuses from the reducing sediments toward the overlying water. The data set is consistent with laboratory studies of sulfide oxidation<sup>5</sup> that show formation of polysulfides early in the oxidation and production of thiosulfate later. In Fig. 3, polysulfides but not thiosulfate are observed deep in the mat whereas thiosulfate but not polysulfides are observed nearer the mat surface.

While colorimetric analyses<sup>25,26</sup> have been employed to measure sulfur species such as thiosulfate, tetrathionate and polysulfides in lab cultures and processed microbial mat cores on thick films that could be cut and analyzed, this is the first report of *in situ* sulfur species other than  $\text{H}_2\text{S}$  in a microbial mat and their occurrence occurs where predicted. The oxidation appears primarily due to biological processes because no metals

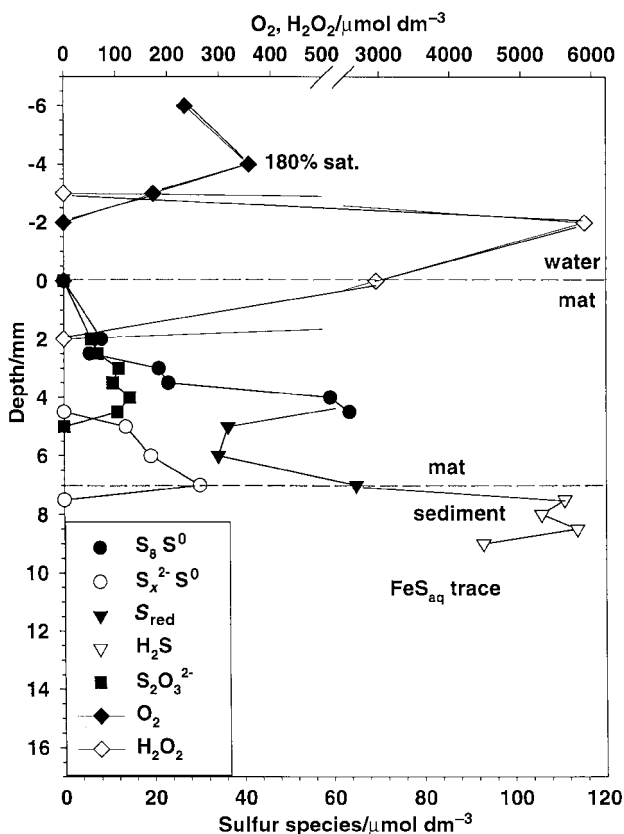


**Fig. 3** Profile of all chemical components measured in the microbial mat. When a chemical species is no longer detected, it is not plotted.  $S_{\text{red}}$  is the peak at  $-0.58 \text{ V}$  and is the sum of all sulfur in the 2-oxidation state from polysulfides and  $\text{H}_2\text{S}/\text{HS}^-$  and in the 0 oxidation state from  $\text{S}_8$ . Note that the data points for these are connected in the figure to show the transition from  $\text{S}_8$  to  $\text{S}_x^{2-}$  to  $\text{H}_2\text{S}$ .

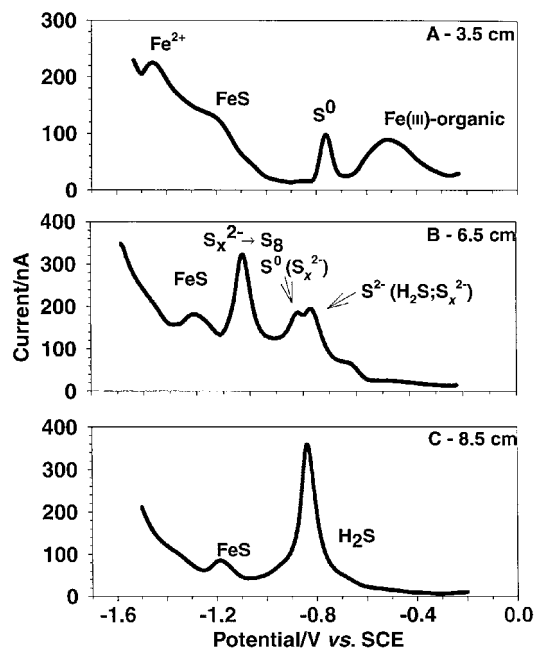


**Fig. 4** Representative CV scans showing sulfur speciation from a subtidal sediment. A,  $1000 \text{ mV s}^{-1}$  scan rate of the upper zone showing  $\text{Fe(III)}$ ,  $\text{S}_8$ ,  $\text{FeS}_{\text{aq}}$ ; B,  $1000 \text{ mV s}^{-1}$  scan rate of the middle area showing the  $\text{S}_x^{2-}$  signals from  $\text{S}^0$  and  $\text{S}^{2-}$ ; C,  $1000 \text{ mV s}^{-1}$  scan rate showing only  $\text{H}_2\text{S}$  and  $\text{FeS}_{\text{aq}}$  as the major components.

(Fe, Mn), which could oxidize sulfide, were detected and O<sub>2</sub> did not co-exist with H<sub>2</sub>S.

### Subtidal sediment work

Similar sulfur speciation was also found in subtidal sediments (Fig. 4) from Rehoboth Bay, Delaware. In these submersed sediments, there are no bacterial mats present and O<sub>2</sub> penetrates to only about 2 mm throughout the year. Sulfate reduction does occur and the resulting sulfide reacts with Fe(III) and Mn(IV) phases, which range in concentration from 10 to 100 μmol (g dry wt)<sup>-1</sup>, to produce partially oxidized sulfur species since O<sub>2</sub> does not penetrate deeply. During Spring, similar speciation was found in these sediments as in the mats except that the sulfur species were found very deep into the core where Fe chemistry dominates. An upper zone consisted primarily of S<sub>8</sub>, and dissolved Fe phases including Fe<sup>2+</sup>, FeS<sub>aq</sub> and Fe(III)-organic complexes. Soluble Fe(III) phases have been found in previous porewater studies.<sup>27</sup> A middle zone consisted of S<sub>x</sub><sup>2-</sup> and FeS<sub>aq</sub>, and finally, a lower completely reduced zone composed of H<sub>2</sub>S/HS<sup>-</sup> and FeS<sub>aq</sub>. The middle zone of polysulfides was only about 5 mm over the 8 cm depth range measured as compared to 4 mm over a 2 cm microbial mat studied. Interestingly a large peak near -0.95 V was also observed in the sediments. We have only been able to reproduce this signal in laboratory solutions of polysulfides that are allowed to oxidize slowly in air. As the oxidation proceeds, white and yellow forms of elemental sulfur are visible in the solution. We hypothesize that the excess elemental sulfur adsorbs to the Hg electrode and interacts with the polysulfide in a donor-acceptor complex (S<sub>x</sub><sup>2-</sup>→S<sub>8</sub> or HS<sup>-</sup>→S<sub>8</sub>) that gives rise to the signal.

Although Fe(III) and Mn(IV) solid phases are present in abundance [total of ~100 μmol (g dry wt)<sup>-1</sup>] in these sediments, solid phases are less reactive than soluble compounds.<sup>3,27</sup> Thus, the combination of slower solid phase reactivity and less microbial oxidation relative to microbial mats provides less dramatic sulfur speciation in these subtidal sediments than in the salt marsh mats. The measurement of dissolved Fe compounds in these subtidal porewaters is in contrast to the salt marsh mat work described above and clearly shows that Fe chemistry is not an important component of mat biogeochemistry. Fe<sup>2+</sup> also reacts quickly with polysulfides and at high micromolar (μmol dm<sup>-3</sup>) concentrations reacts to form FeS and S<sub>8</sub>.<sup>7</sup> Thus, polysulfides should not reach high levels when dissolved metals are present.

### In situ hydrothermal vent work

In order to assess sulfur speciation at vents, we placed the sensor package near the plumes of the vent tubeworms *Riftia pachyptila*, which reside in diffuse flow waters at the base or on the lower walls of the vents. These tubeworms grow up to 2 m tall and harbor bacterial endosymbionts. The primary source of organic carbon for their growth is from the bacterially mediated chemosynthetic reaction of H<sub>2</sub>S/HS<sup>-</sup> with CO<sub>2</sub> by the endosymbionts, and the *R. pachyptila* move their plumes into diffuse flow waters that contain H<sub>2</sub>S/HS<sup>-</sup>. However, the formation of S<sub>8</sub> from chemosynthesis occurs within the bacteria residing in *R. pachyptila* not outside *Riftia*. For partially oxidized sulfur species to form in the vent waters around *R. pachyptila*, oxygen or Fe(III) formed from Fe(II) oxidation by oxygen must react with H<sub>2</sub>S, both H<sub>2</sub>S and Fe(II) diffuse from the vent area.

Figs. 5A and B show CV data and Fig. 5C time course data over a 2.5 min period at 8.5 °C. Fig. 6 shows the sensor package in one of the manipulators of DSV *Alvin* above *R. pachyptila*. The first scans showed that O<sub>2</sub> and H<sub>2</sub>S co-exist whereas later on in the *in situ* experiment, the sulfide peak split into two peaks indicating that polysulfides formed. S<sup>0</sup> from polysulfides

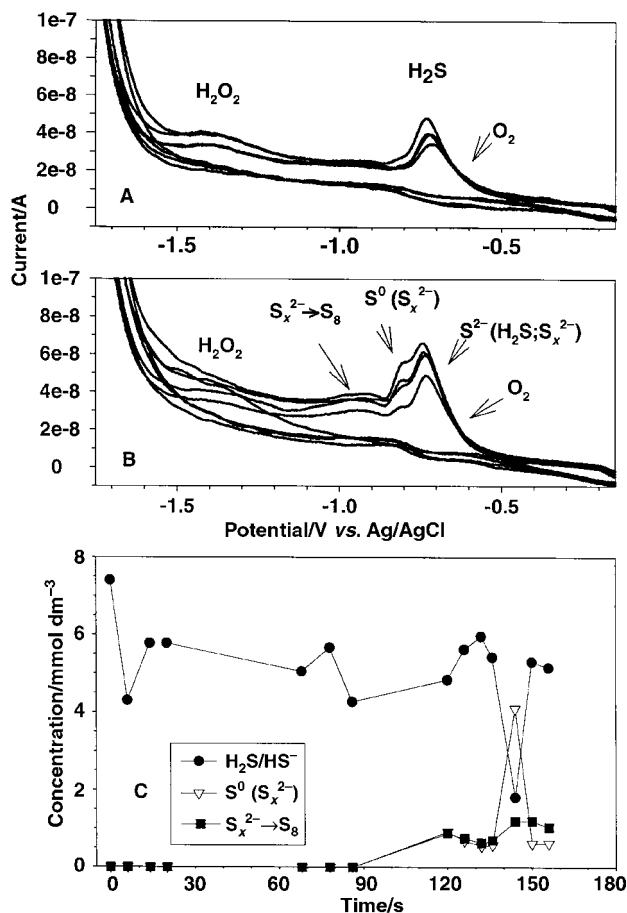


**Fig. 5** Representative CV scans showing sulfur speciation from diffuse flow area near the vent tubeworms *R. pachyptila*. A, Initial 1000 mV s<sup>-1</sup> scans showing that only O<sub>2</sub> and H<sub>2</sub>S co-exist; B, subsequent 1000 mV s<sup>-1</sup> scans showing that O<sub>2</sub>, H<sub>2</sub>S and S<sub>x</sub><sup>2-</sup> signals from S<sup>0</sup> and S<sup>2-</sup> are observable; C, time course showing the rapid change in sulfur speciation at the tubeworm location.

typically are about 25% or less of the total S found near the plumes so that the S<sup>2-</sup> sulfur due to H<sub>2</sub>S/HS<sup>-</sup> is about 70% of the total sulfur measured. The sulfur speciation changed in a matter of seconds and indicates that O<sub>2</sub> is not the direct oxidant of H<sub>2</sub>S under diffuse flow conditions. Fe is in trace quantities (~1 μmol dm<sup>-3</sup>) in these diffuse flow waters as determined by analysis of discrete samples onboard ship using the Fe-

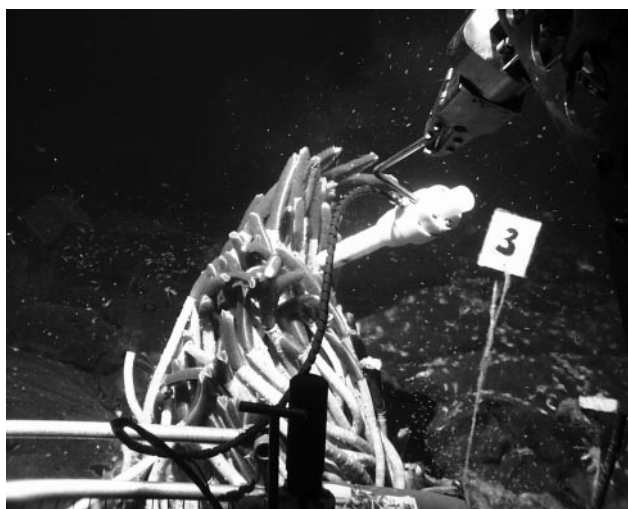


**Fig. 6** Deployment of the sensor package above *R. pachyptila*. (For a colour version of this figure see Electronic Supplementary Information.<sup>1‡</sup>)

ferrozine assay.<sup>28</sup> The pH of these waters is typically between 6 and 6.8 where Fe<sup>2+</sup> oxidation by O<sub>2</sub> is faster than H<sub>2</sub>S oxidation by O<sub>2</sub>.<sup>29,30</sup> Moreover, Fe(III) formed from the reaction of Fe(II) with O<sub>2</sub> is the likely oxidant because the transfer of a single electron from H<sub>2</sub>S to O<sub>2</sub> is thermodynamically unfavorable<sup>31</sup> and Fe<sup>2+</sup> catalysis of sulfide oxidation in oxygenated waters is very fast.<sup>32</sup> The Fe(III), which formed in real time, is likely a soluble form that is very reactive<sup>27</sup> and can produce polysulfides in a matter of seconds. Thiosulfate, if present, was below the detection limit in these waters.

## Conclusions

The sulfur compounds of intermediate oxidation state (which are typically found in microbial mats, subtidal sediments, and hydrothermal vent waters above the electrode's detection limits) are thiosulfate, polysulfides and aqueous elemental sulfur. Trace amounts of tetrathionate (data not shown) have also been detected. These partially oxidized sulfur species are found at redox transition zones where both an oxidant (e.g., O<sub>2</sub>) and a reductant (e.g., H<sub>2</sub>S) can be found or where biological mediation can occur. Fe(III) phases are important in the oxidation of H<sub>2</sub>S and can form quickly as dissolved components when O<sub>2</sub> and Fe<sup>2+</sup> react in waters of pH > 6. The major reduced dissolved sulfur species found are hydrogen sulfide and/or aqueous iron monosulfide; thiols were not detected in these study areas. In microbial mats, our data confirms that Fe and Mn chemistry are not significant in the oxidation of H<sub>2</sub>S. Because these measurements were made in real time and in the field without sample processing and/or manipulation, sulfur speciation is caused by *in situ* biogeochemical processes and is not due to artefacts. Polysulfides are the first detected sulfur species during H<sub>2</sub>S oxidation in these field studies and can form in seconds to minutes at circumneutral pH when dissolved Fe and O<sub>2</sub> coexist as in hydrothermal vent diffuse flow waters.

## Acknowledgements

This work was supported by grants from the National Oceanic and Atmospheric Administration (NA16RG0162-03), the National Science Foundation (OCE-9714302) and a NSF Postdoctoral award to T.F. Rozan. We would like to thank David Rickard and Anthony Oldroyd for providing us with pure sodium tetrasulfide, and S. Craig Cary for contributions to our hydrothermal vent work.

## References

- 1 W. Yao and F. J. Millero, *Geochim. Cosmochim. Acta*, 1993, **57**, 3359.
- 2 W. Yao and F. J. Millero, *Mar. Chem.*, 1996, **52**, 1.
- 3 M. dos Santos Afonso and W. Stumm, *Langmuir*, 1992, **8**, 1671.
- 4 M. R. Hoffmann, *Environ. Sci. Technol.*, 1977, **11**, 61.
- 5 K. Y. Chen and J. C. Morris, *Environ. Sci. Technol.*, 1972, **6**, 529.
- 6 B. B. Jørgensen, *Science*, 1990, **249**, 152.
- 7 S. J. Chadwell, D. Rickard and G. W. Luther, III, *Aquat. Geochem.*, 1999, **5**, 29.
- 8 A. Vairavamurthy and K. Mopper, in *Biogenic Sulfur in the Environment*, ed. E. Saltzmann and W. J. Copper, ACS, Washington, DC, 1989, vol. 393, ch. 15, pp. 231–242.
- 9 R. T. Lalonde, L. M. Ferrara and M. P. Hayes, *Org. Geochem.*, 1987, **11**, 563.
- 10 G. W. Luther, III, A. E. Giblin and R. Varsolona, *Limnol. Oceanogr.*, 1985, **30**, 727.
- 11 G. W. Luther, III, T. E. Church, A. E. Giblin, and R. W. Howarth, in *Organic Marine Geochemistry*, ed. M. Sohn, ACS, Washington, DC, 1986, vol. 305, ch. 20, pp. 340–355.
- 12 S. M. Theberge and G. W. Luther, III, *Aquat. Geochem.*, 1997, **3**, 191.
- 13 N. Batina, I. Cigenecki and B. Cosovic, *Anal. Chim. Acta*, 1992, **267**, 157.
- 14 I. Ciglenečki and B. Čosović, *Electroanalysis*, 1997, **9**, 775.
- 15 F. A. Wang, Tessier and J. Buffle, *Limnol. Oceanogr.*, 1998, **43**, 1353.
- 16 T. F. Rozan, S. M. Theberge and G. W. Luther, III, *Anal. Chim. Acta*, 2000, **415**, 175.
- 17 J. Jordan, J. Talbott and J. Yakupkovic, *Anal. Lett.*, 1989, **22**, 1537.
- 18 P. J. Brendel and G. W. Luther, III, *Environ. Sci. Technol.*, 1995, **29**, 751.
- 19 G. W. Luther, III, C. E. Reimers, D. B. Nuzzio and D. Lovalvo, *Environ. Sci. Technol.*, 1999, **33**, 4352.
- 20 C. A. Di Meo, J. R. Wakefield and S. C. Cary, *Deep-Sea Res., Part I*, 1999, **46**, 1279.
- 21 A. M. Bond, *Modern Polarographic Methods in Analytical Chemistry*, Marcel Dekker, New York, 1980.
- 22 K. Xu, S. C. Dexter and G. W. Luther, III, *Corrosion*, 1998, **54**, 814.
- 23 H. van Gemerden, *Mar. Geol.*, 1993, **113**, 3.
- 24 N. P. Revsbech and B. B. Jørgensen, *Limnol. Oceanogr.*, 1983, **28**, 749.
- 25 F. van den Ende and H. Van Gemerden, *FEMS Microbiol. Ecol.*, 1993, **13**, 69.
- 26 P. T. Visscher, J. W. Nijurg and H. Van Gemerden, *Arch. Microbiol.*, 1990, **155**, 75.
- 27 M. Taillefert, A. B. Bono and G. W. Luther, III, *Environ. Sci. Technol.*, 2000, **34**, 2169.
- 28 L. L. Stookey, *Anal. Chem.*, 1970, **41**, 779.
- 29 F. J. Millero, S. Hubinger, M. Fernandez and S. Garnett, *Environ. Sci. Technol.*, 1987, **21**, 439.
- 30 F. J. Millero, S. Sotolongo and M. Izaguirre, *Geochim. Cosmochim. Acta*, 1987, **51**, 793.
- 31 G. W. Luther, III and T. G. Ferdelman, *Environ. Sci. Technol.*, 1993, **27**, 1154.
- 32 F. G. Vazquez, J. Zhang and F. J. Millero, *Geophys. Res. Lett.*, 1989, **16**, 1363.